TABLE 3. Comparison of BceICT with BcICT and BeICT in the detection of specific antibodies against *B. caballi* and *B. equi* infections in field sera

BcICT or BeICT detection result	BceICT detection of antibodies specific for[a]:			
	Anti-*B. caballi* antibody		Anti-*B. equi* antibody	
	No. of positive sera (%)	No. of negative sera (%)	No. of positive sera (%)	No. of negative sera (%)
BcICT				
+	18 (32.1)	1 (1.8)		
−	0	37 (66.1)		
BeICT				
+			26 (46.4)	0
−			1 (1.8)	29 (51.8)
Total (n = 56)	18 (32.1)	38 (67.9)	27 (48.2)	29 (51.8)

[a] The percentage of results that corresponded with those of BceICT was 98.2% for both BcICT and BeICT.

phase, which are conjugated with gold particles, and antigens and antibodies in the immobile phase. The captured antigen and antibody complex then develops a colored line. As soon as the test strip is available, the performance is as simple as loading the sample onto the strip, and the result can be determined in a few minutes with the naked eye, according to the colored lines. No equipment or testing skills are required. Therefore, this test is more practical to use in the field than any other test. In our previous studies, the BcICT and BeICT were developed for the detection of antibodies to *B. caballi* (unpublished data) and *B. equi* (6). Both of the tests showed results that were comparable with those of ELISAs. To combine the two ICTs into one test, we developed a BceICT for the simultaneous detection of antibodies against infection by two species of *Babesia*. Using this test, some materials used for the preparation of test strips, sera, manpower, and time required could be reduced by one-half.

Detection results of the specific antibodies in the known *B. caballi*- and *B. equi*-infected and uninfected horses indicate that the sensitivity and specificity of the BceICT was 83.3% and 92.9%, respectively, for anti-*B. caballi* antibody and 94.1% and 88.2%, respectively, for anti-*B. equi* antibody. No significant differences were observed in sensitivity between BceICT and BcELISA and between BceICT and BeELISA. However, the specificity of the BceICT was less than those of BcELISA and BeELISA. The nonspecific reaction in the BceICT for the detection of *B. equi* infection was observed mainly in sera from *B. caballi*-infected horses, in reverse, and that for the detection of *B. caballi* infection was observed mainly in sera from *B. equi*-infected horses. Therefore, these nonspecific reactions may be due to an antigen or antibody cross-reaction rather than the effect of some physical or chemical factors. The reaction may occur when the two conjugates are mixed. Other possibilities are related to the storage of the sera, for example, the length of the storage period, the quantity of preservative added, or the conditions for the preparation of the test strips. If further discrimination between the two species is necessary, ELISAs could be carried out to examine the BceICT-positive sera.

The high correspondence of BceICT results with ICT or ELISA results were also found for *B. caballi* and *B. equi* infections, respectively, in sera collected from horses in the field. The correspondence of the BceICT with BcELISA, BeELISA, BcICT, and BeICT were 91.8%, 95.9%, 98.2%, and 98.2%, respectively (Tables 1, 2, and 3). These results for *B. equi* infection were very comparable with those in previous studies (6).

In conclusion, the present study indicates that the BceICT employing antigen bound to nitrocellulose membranes has a high specificity and sensitivity for detecting antibodies to both *B. caballi* and *B. equi*. The results of the BceICT are easily obtained and comparable with those from ELISA. Therefore, the BceICT is a feasible field test for the simultaneous serodiagnosis of both types of equine babesiosis, even though some improvements of the BceICT and an evaluation on a larger scale are necessary.

ACKNOWLEDGMENTS

This study was supported by grants from the 21st Century COE Program (A-1) and Ministry of Education, Culture, Sports, Science, and Technology, Japan, and by Grants-in-Aid for Scientific Research from the Japan Society for the Promotion of Science.

REFERENCES

1. **Bruning, A.** 1996. Equine piroplasmosis: an update on diagnosis, treatment, and prevention. Br. Vet. J. **152**:139–151.
2. **de Waal, D. T.** 2000. Global importance of piroplasmosis. J. Protozool. Res. **10**:106–127.
3. **Hirata, H., H. Ikadai, N. Yokoyama, X. Xuan, K. Fujisaki, N. Suzuki, T. Mikami, and I. Igarashi.** 2002. Cloning of a truncated *Babesia equi* gene encoding an 82-kilodalton protein and its potential use in an enzyme-linked immunosorbent assay. J. Clin. Microbiol. **40**:1470–1474.
4. **Holbrook, A. A.** 1969. Biology of equine piroplasmosis. J. Am. Vet. Med. Assoc. **155**:453–454.
5. **Huang, X., X. Xuan, N. Yokoyama, L. Xu, H. Suzuki, C. Sugimoto, H. Nagasawa, K. Fujisaki, and I. Igarashi.** 2003. High-level expression and purification of a truncated merozoite antigen-2 of *Babesia equi* in *Escherichia coli* and its potential for immunodiagnosis. J. Clin. Microbiol. **41**:1147–1151.
6. **Huang, X., X. Xuan, L. Xu, S. Zhang, N. Yokoyama, N. Suzuki, and I. Igarashi.** 2004. Development of an immunochromatographic test with recombinant EMA-2 for the rapid detection of antibodies against *Babesia equi* in horses. J. Clin. Microbiol. **42**:359–361.
7. **Ikadai, H., X. Xuan, I. Igarashi, S. Tanaka, T. Kanemaru, H. Nagasawa, K. Fujisaki, N. Suzuki, and T. Mikami.** 1999. Cloning and expression of a 48-kilodalton *Babesia caballi* merozoite rhoptry protein and potential use of the recombinant antigen in an enzyme-linked immunosorbent assay. J. Clin. Microbiol. **37**:3475–3480.
8. **Ikadai, H., C. R. Osorio, X. Xuan, I. Igarashi, H. Nagasawa, K. Fujisaki, N. Suzuki, and T. Mikami.** 2000. Detection of *Babesia caballi* infection by enzyme-linked immunosorbent assay using recombinant 48-kDa merozoite rhoptry protein. Int. J. Parasitol. **30**:633–635.
9. **Knowles, D. P., Jr., L. E. Perryman, L. S. Kappmeyer, and S. G. Hennager.** 1991. Detection of equine antibody to *Babesia equi* merozoite proteins by a monoclonal antibody-based competitive inhibition enzyme-linked immunosorbent assay. J. Clin. Microbiol. **29**:2056–2058.
10. **Tanaka, T., X. Xuan, H. Ikadai, I. Igarashi, H. Nagasawa, K. Fujisaki, T. Mikami, and N. Suzuki.** 1999. Expression of *Babesia equi* merozoite antigen-2 by recombinant baculovirus and its use in the ELISA. Int. J. Parasitol. **29**:1803–1808.
11. **Tenter, A. M., and K. T. Friedhoff.** 1986. Serodiagnosis of experimental and natural *Babesia equi* and *B. caballi* infections. Vet. Parasitol. **20**:49–61.
12. **Weiland, G.** 1986. Species-specific serodiagnosis of equine piroplasma infections by means of complement fixation test, immunofluorescence, and enzyme-linked immunosorbent assay. Vet. Parasitol. **20**:43–48.
13. **Xuan, X., A. Larsen, H. Ikadai, T. Tanaka, I. Igarashi, H. Nagasawa, K. Fujisaki, Y. Toyoda, N. Suzuki, and T. Mikami.** 2001. Expression of *Babesia equi* merozoite antigen 1 in insect cells by recombinant baculovirus and evaluation of its diagnostic potential in an enzyme-linked immunosorbent assay. J. Clin. Microbiol. **39**:705–709.
14. **Xuan, X., A. Nagai, B. Battsetseg, S. Fukumoto, L. H. Makala, N. Inoue, I. Igarashi, T. Mikami, and K. Fujisaki.** 2001. Diagnosis of equine piroplasmosis in Brazil by serodiagnostic methods with recombinant antigens. J. Vet. Med. Sci. **63**:1159–1160.

Available online at www.sciencedirect.com
ScienceDirect
Veterinary Parasitology 143 (2007) 155–160
veterinary parasitology
www.elsevier.com/locate/vetpar

Short communication

Development of loop-mediated isothermal amplification (LAMP) method for diagnosis of equine piroplasmosis

Andy Alhassan [a], Oriel M.M. Thekisoe [a], Naoaki Yokoyama [a], Noboru Inoue [a], Makhosazana Y. Motloang [b], Peter A. Mbati [b], Hong Yin [c], Yoshinari Katayama [d], Toru Anzai [d], Chihiro Sugimoto [a,e], Ikuo Igarashi [a,*]

[a] *National Research Center for Protozoan Diseases, Obihiro University of Agriculture and Veterinary Medicine, Inada-cho, Obihiro, Hokkaido 080-8555, Japan*
[b] *Parasitology Research Program, University of the Free State QwaQwa Campus, Phuthaditjhaba 9866, South Africa*
[c] *Lanzhou Veterinary Research Institute, Chinese Academy of Agricultural Sciences, Lanzhou, Gansu 730046, People's Republic of China*
[d] *Epizootic Research Station, Equine Research Institute, Japan Racing Association, Kokubunji, Tochigi 329-0412, Japan*
[e] *Research Center for Zoonosis Control, Hokkaido University, Sapporo, Hokkaido 060-0818, Japan*

Received 1 March 2006; received in revised form 22 July 2006; accepted 3 August 2006

Abstract

Loop-mediated isothermal amplification (LAMP) is a novel nucleic acid method whereby DNA is amplified with high specificity, efficiency, and rapidity under isothermal conditions using a set of four specifically designed primers and a DNA polymerase with strand displacement activity. In this study, we used LAMP primer sets designed from EMA-1 and Bc 48 genes for detection of *Theileria equi* and *Babesia caballi* infections, respectively. These primer sets specifically amplified DNA of the respective parasites. Both primer sets amplified *T. equi* and *B. caballi* up to 10^{-6} dilution of 10-fold serially diluted samples. Furthermore, DNA extracted from blood collected from a horse experimentally infected with *T. equi* was amplified by a *T. equi* LAMP primer set from days 2 to 35 post-infection, demonstrating the high sensitivity of these primers. Of 55 samples collected from China, 81.8% and 56.3% were positively detected by LAMP for *T. equi* and *B. caballi* infections, respectively. In contrast, 91.8% and 45.9% of the 37 samples collected from South Africa were LAMP positive for *T. equi* and *B. caballi*, respectively. These results suggest that LAMP could be a potential diagnostic tool for epidemiological studies of equine piroplasmosis.

Keywords: Equine piroplasmosis; *Theileria equi*; *Babesia caballi*; LAMP; PCR

1. Introduction

Equine piroplasmosis caused by *Theileria equi* (Melhorn and Schein, 1998) and *Babesia caballi* (Schein, 1988), is an economically important protozoan disease of horses in tropical and subtropical regions, including Central and South America, Africa, Asia, and Southern Europe. Ticks belonging to the genera *Boophilus*, *Hyalomma*, *Dermacentor*, and *Rhipicephalus* transmit these parasites (Bruning, 1996; Dash, 1966; Massaro et al., 2003). At present, only USA, Canada, Japan, UK, and Australia are considered equine piroplasmosis-free and have in place stringent regulatory import restrictions to prevent introduction of these parasites (Friedhoff et al., 1990).

* Corresponding author. Tel.: +81 155 49 5641; fax: +81 155 49 5643.
E-mail address: igarcpmi@obihiro.ac.jp (I. Igarashi).

0304-4017/$ – see front matter © 2006 Elsevier B.V. All rights reserved.
doi:10.1016/j.vetpar.2006.08.014

While the identification of parasites in blood smears constitutes the definitive diagnosis of equine infection, it bears certain limitations, particularly during apparent or chronic infection due to low parasitemias (Krause et al., 1996). Thus, several serological assays such as ELISA and molecular tools that are often more sensitive and specific have been developed to advance diagnosis of equine piroplasmosis (Nicolaiewsky et al., 2001; Xuan et al., 2001). Among the molecular tools, PCR is the most commonly used, including other PCR-derived tools, such as the multiplex and nested PCR (Fahrimal et al., 1992; Alhassan et al., 2005). However, these molecular tools require thermo cyclers and several other expensive operations, which make them unsuitable for routine diagnosis, especially in resource-poor countries.

Recently, introduction of loop-mediated isothermal amplification (LAMP) has resulted in development of another rapid, sensitive, and specific diagnostic method (Notomi et al., 2000), and is already developed for detection of several viral, bacterial, and protozoan infections (Enosawa et al., 2003; Kuboki et al., 2003; Ihira et al., 2004). As such, LAMP is a desirable and practicable alternative to standard PCR for routine diagnosis of equine babesiosis. In the present study, we developed a LAMP method for the diagnosis of *T. equi* and *B. caballi* and evaluated its sensitivity and specificity with blood samples obtained from experimentally infected and field horses.

2. Materials and methods

2.1. Parasites

USDA strains of *T. equi* and *B. caballi* parasites were grown in equine red blood cells using a previously established continuous microaerophilous stationary-phase culture system (Avarzed et al., 1997). *T. equi* and *B. caballi*-infected erythrocytes with 5% parasitemia were subjected to 10-fold dilutions in normal equine blood, and DNA extracted from each diluted sample for sensitivity test. Additionally, *T. equi* and *B. caballi* infected blood was blotted and dried on filter papers (FTA card®, Whatman, UK), and used as positive controls whilst purified DNA from uninfected horse blood, *Babesia bovis* and *Trypanosoma evansi* infected blood also blotted on filter papers were used as negative controls.

2.2. Blood samples and DNA extraction

Nineteen blood samples from an experimentally infected horse were obtained from Japan Racing Association (JRA), Tochigi, Japan. The horse was inoculated intravenously with 10 ml of *T. equi* infected blood and bled every 2 days for a period of 35 days. Blood samples were collected from the jugular vein into vacutainer tubes with EDTA and stored at −20 °C until use. In addition, 55 and 37 blood samples were collected on filter papers (Whatman) from horses in China (Gansu Province) and South Africa (Eastern Free State Province), respectively. DNA was extracted from *in vitro* cultured parasites as described by Alhassan et al. (2005). Blood blotted filter papers (Whatman) from field samples were purified according to manufactures instructions.

2.3. Microscopy and ELISA

Parasitemia was monitored daily by Giemsa-stained thin blood smear whilst ELISA was performed using recombinant EMA-1 antigen as described by Xuan et al. (2001).

2.4. LAMP and PCR reaction

LAMP specific primers for *T. equi* and *B. caballi* (Table 1) were designed against the EMA-1 (accession number AB043618) and Bc48 (accession number AB017700) genes, respectively, using the LAMP Primer Explorer program V2 (Fujitsu, Japan). The LAMP reaction was conducted as described previously (Notomi et al., 2000). Briefly, the reaction was performed in 25 μl of a mixture containing 12.5 μl LAMP buffer (20 mM Tris–HCl (pH 8.8), 10 mM KCl, 8 mM $MgSO_4$, 10 mM $(NH_4)_2SO_4$, 0.8 M betaine, and 1.4 mM concentration of each deoxynucleoside triphosphate (dNTP), Sigma, Japan), 2 μl of extracted DNA or a piece of filter paper, 40 pmol each of primers FIP and BIP, 5 pmol each of primers F3 and B3, and 1 μl of

Table 1
LAMP primers designed for *T. equi* and *B. caballi*

Parasite	Primer set	Sequence
Theileria equi	BEQ1	F3: TTGCCATTTCGAGCATCCT B3: ACGGTCTTTGGGGTATGTTC FIP: TGCTTGTCGATGGTGATGTGGT-AGGAGGAGAAACCCAAGGC BIP: GTCCGAGGAGCACGTCGTCTA-GTCTTGATGACGGAGTCGC
Babesia caballi	BCAB1	F3: TGTTTCCATCATGGCTCCC B3: GCGCTAACGGAAGCACTG FIB: GGCATTGGCAGCTGAGTCCA-GGCGACGTGACTAAGACCT BIP: AGCGATTACTTGTCGGCTGTGT-CCCCTTAGGGACCTGACTG

Bst DNA polymerase. The mixture was incubated in a heat block, at 63 °C for 60 min and, subsequently, at 80 °C for 2 min to terminate the reaction. The LAMP products were subjected to electrophoresis on 1.5% agarose gel in a Tris–acetic acid–EDTA (TAE) buffer and visualized under a UV light after staining with ethidium bromide.

The outer LAMP primer pairs designated F3 and B3 for *T. equi* and *B. caballi*, respectively, were used for PCR amplification as described by Ikadai et al. (2004). PCR products were analyzed by electrophoresis and visualized as described above for LAMP products.

3. Results

3.1. Specificity and sensitivity of LAMP and PCR

Application of LAMP specific primers to *T. equi* and *B. caballi* DNA resulted in successful amplification of the target genes of the respective parasites whereby positive LAMP products demonstrated a typical ladder pattern (Fig. 1A and B). Similar results were observed in PCR with B3 and F3 primers, where single bands of 200 and 180 bp were identified for *T. equi* and *B. caballi*, respectively (Fig. 2). Furthermore, LAMP and PCR methods were equally sensitive, detecting up to 10^{-6} dilution of *T. equi* and *B. caballi* DNA (data not shown). In the *T. equi* experimentally infected horse, microscopy detected parasites 4 days p.i., whilst antibodies against *T. equi* were detected 6 days p.i. However, LAMP and PCR detected *T. equi* DNA from 2 days p.i. (Table 2).

3.2. Detection of T. equi and B. caballi from field samples

Field samples collected from China (Gansu Province) and South Africa (Eastern Free State Province) were screened using the LAMP method in order to demonstrate the ability of LAMP as a diagnostic tool for epidemiological studies. As shown in Table 3, the infection rates for *B. equi* were 81.8% (China) and 91.8% (South Africa), whilst the infection rates for *B. caballi* were 45.9% (China) and 56.3% (South Africa). In addition, mixed infection rates of *T. equi* and *B. caballi* were 40.5% (China) and 49% (South Africa). PCR could not detect infections from filter papers.

4. Discussion

In this report, we describe the development of loop-mediated isothermal-amplification (LAMP) method for diagnosis of *T. equi* and *B. caballi* using species-specific EMA-1 and Bc48 genes, respectively (Knowles et al., 1991; Ikadai et al., 1999). LAMP primer sets designed from the above mentioned genes specifically amplified the respective parasite DNA. These findings are in agreement with previous reports that the specificity of LAMP method in detection of protozoan parasites such as Trypanosomes and *Babesia gibsoni* is extremely high (Kuboki et al., 2003; Ikadai et al., 2004). This is because LAMP employs four primers (FIP, BIP, F3, and B3) that recognize six sequences on the target DNA, thereby

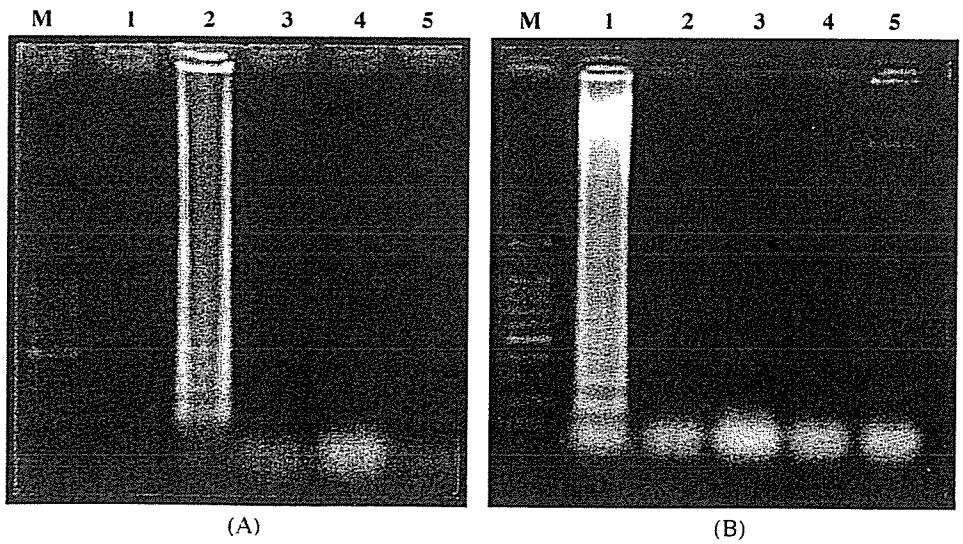

Fig. 1. Specificity of LAMP primers for the detection of *Theileria equi* and *Babesia caballi*. (A) *T. equi* LAMP primers (BEQ1). Lanes (M) 100 bp DNA ladder; (1) normal horse DNA; (2) *T. equi*; (3) *B. caballi*; (4) *B. bovis*; (5) *T. evansi* DNA. (B) *B. caballi* LAMP primers (BCAB1). Lanes (M) 100 bp DNA ladder; (1) *B. caballi* DNA; (2) *T. equi*; (3) *B. bovis*; (4) *T. evansi*; (5) normal horse DNA.

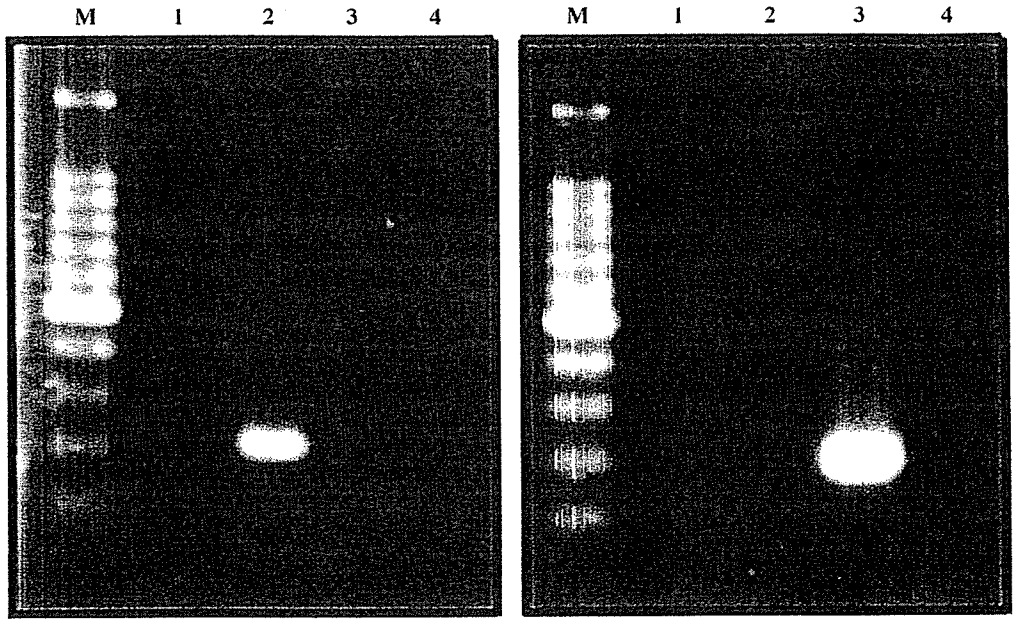

Fig. 2. PCR amplification of *T. equi* and *B. caballi* with specific LAMP B3 and F3 primers, respectively. (A) *T. equi* primers (B3 and F3). Lanes (M) 100 bp DNA ladder; (1) normal horse DNA; (2) *T. equi*; (3) *B. caballi*; (4) *B. bovis* DNA. (B) *B. caballi* primers (B3 and F3). Lanes (M) 100 bp DNA ladder; (1) normal horse DNA; (2) *T. equi*; (3) *B. caballi*; (4) *B. bovis* DN.

ensuring high specificity (Notomi et al., 2000). LAMP is a highly sensitive method whereby DNA with as few as six copies can be detected in a reaction mixture. In addition, its cycling reaction continues for 1 h with the accumulation of 10^9 of the target DNA (Notomi et al., 2000). In this study, sensitivity of the LAMP method proved to be high for both *T. equi* and *B. caballi* serially diluted DNA obtained from *in vitro* cultures.

Table 2
Detection of *T. equi* infection by microscopy, ELISA, PCR and LAMP in experimentally infected horse

Days p.i.	Microscopy	ELISA	PCR	LAMP
0	–	–	–	–
2	–	–	+	+
4	+	–	+	+
6	+	+	+	+
8	+	+	+	+
10	+	+	+	+
12	+	+	+	+
14	+	+	+	+
16	+	+	+	+
18	–	+	+	+
20	–	+	+	+
22	+	+	+	+
24	+	+	+	+
26	+	+	+	+
28	+	+	+	+
30	+	+	+	+
32	–	+	+	+
34	–	+	+	+
35	–	+	+	+

Furthermore, in sequential blood samples from a horse experimentally infected with *T. equi*, LAMP and PCR detected the parasite DNA from early stages of infection as compared to microscopy and ELISA (Table 1).

The current study has further applied LAMP in epidemiological studies on field samples collected on filter papers from China and South Africa. Our results confirm previous reports that both *T. equi* and *B. caballi* exist in China (Xu et al., 2003) and South Africa (Gummow et al., 1996). It is noteworthy that, results of this study do not represent the current epidemiological status in these countries because the samples were collected from small regions of each country. However, all samples on filter papers were negative by PCR. It has been previously reported that PCR has poor sensitivity for amplification of DNA on filter papers as compared to LAMP (Kuboki et al., 2003). We believe that this is due to blood components

Table 3
Detection of equine vpiroplasmosis by LAMP method from field samples

Source	# Blood samples	# Positive (%)		
		T. equi	*B. caballi*	Mixed infection
China	55	45 (81.8)	31 (56.3)	27 (49.0)
South Africa	37	34 (91.8)	17 (45.9)	15 (40.5)

such as myoglobin, hem-blood protein complexes and immunoglobulin G which inactivates Taq DNA polymerase used in standard PCR. In contrast, such inhibitors do not affect the *Bst* polymerase used in LAMP (Grab et al., 2005).

One of the reasons that molecular diagnostic methods, particularly, DNA extraction methods have not been widely used for clinical diagnosis and epidemiological studies despite their reported specificity and sensitivity, especially in resource-poor countries, is the fact that they are considered to be complicated (Eisler et al., 2004). LAMP amplifies DNA from purified filter papers, with ease. This, together with LAMP's advantages of simplicity whereby the reaction is conducted within an hour and that LAMP products can be observed by naked eye from turbidity (Mori et al., 2001), should enable LAMP to be applied as a rapid molecular diagnostic tool even in resource poor countries.

Acknowledgments

We thank the Japan Racing Association (JRA) for providing the samples experimentally infected with *T. equi* for this study. We also thank the horse farmers in China and South Africa for their cooperation. This study was supported by Grants-in-Aid for Young Scientists, Grants-in-Aid for Scientific Research from the Japan Society for the Promotion Science and from the 21st Century COE program (A-1), Ministry of Education, Sports, Science, and Technology of Japan.

References

Alhassan, A., Pumidonming, W., Okamura, M., Hirata, H., Battsetseg, B., Fujisaki, K., Yokoyama, N., Igarashi, I., 2005. Development of a single-round and multiplex PCR method for the simultaneous detection of *Babesia caballi* and *Babesia equi* in horse blood. Vet. Parasitol. 129, 43–49.

Avarzed, A., Igarashi, I., Kanemaru, T., Hirumi, K., Omata, Y., Saito, A., Oyamada, T., Nagasawa, H., Toyoda, Y., Suzuki, N., 1997. Improved *in vitro* cultivation of *Babesia caballi*. J. Vet. Med. Sci. 59, 479–481.

Bruning, A., 1996. Equine piroplasmosis an update on diagnosis, treatment and prevention. Br. Vet. J. 152, 139–151.

Dash, M., 1966. Haemosporidioses of Horses. Khevlekh uildver, Ulaanbaatar, pp. 7–9 (in Russian).

Eisler, M.C., Dwinger, R.H., Majiwa, P.A.O., Picozzi, K., 2004. Diagnosis and epidemiology of African animal trypanosomiasis. In: Maudlin, I., Holmes, P.H., Miles, M.A. (Eds.), The Trypanosomiasis. CABI Publishing, United Kingdom.

Enosawa, M., Kageyama, S., Sawai, K., Watanabe, K., Notomi, T., Onoe, S., Mori, Y., Yokomizo, Y., 2003. Use of loop-mediated isothermal amplification of the IS900 sequence for rapid detection of cultured *Mycobacterium avium* subsp. paratuberculosis. J. Clin. Microbiol. 41, 4359–4365.

Fahrimal, Y., Goff, W.L., Jasmer, D.P., 1992. Detection of *Babesia bovis* carrier cattle by using polymerase chain reaction amplification of parasite DNA. J. Clin. Microbiol. 30, 1374–1379.

Friedhoff, K.T., Tenter, A.M., Muller, I., 1990. Haemoparasites of equines: impact on international trade of horses. Rev. Sci. Technol. 9, 1187–1194.

Grab, J.D., Lonsdale-Eccle, J., Inoue, N., 2005. LAMP for tadpoles. Nat. Methods 2, 635.

Gummow, B., de wet, C.S., de Waal, D.T., 1996. A sero-epidemiological survey of equine piroplasmosis in the northern and eastern Cape Provinces of South Africa. J. S. Afr. Vet. Assoc. 67, 204–208.

Ihira, M., Yoshikawa, T., Enomoto, Y., Akimoto, S., Ohashi, M., Suga, S., Nishimura, N., Ozaki, T., Nishiyama, Y., Notomi, T., Ohta, Y., Asano, Y., 2004. Rapid diagnosis of human herpesvirus 6 infection by a novel DNA amplification method, loop-mediated isothermal amplification. J. Clin. Microbiol. 42, 140–145.

Ikadai, H., Xuan, X., Igarashi, I., Tanaka, S., Kanemuru, T., Nagasawa, H., Fujisaki, K., Suzuki, N., Mikami, T., 1999. Cloning and expression of a 48-kilodalton *Babesia caballi* merozoite rhoptry protein and potential use of the recombinant antigen in an enzyme-linked immunosorbent assay. J. Clin. Microbiol. 37, 3475–3480.

Ikadai, H., Tanaka, H., Shibahara, N., Matsuu, A., Uechi, M., Itoh, N., Oshiro, S., Kudo, N., Igarashi, I., Oyamada, T., 2004. Molecular evidence of infections with *Babesia gibsoni* parasites in Japan and evaluation of the diagnostic potential of a loop-mediated isothermal amplification method. J. Clin. Microbiol. 42, 2465–2469.

Knowles, D.P., Perryman, L.E., Goff, W.L., Miller, C.D., Harrington, R.D., Gorham, J.R., 1991. A monoclonal antibody defines a geographically conserved surface protein epitope of *Babesia equi* merozoites. Infect. Immun. 59, 2412–2417.

Krause, P.J., Speilman, T.A., Ryan, R., Magera, J., Rajan, T.V., Christianson, D., Alberghini, T.V., Bow, L., Persing, D., 1996. Comparison of PCR with blood smear and inoculation of small animals for diagnosis of *Babesia microti* parasitemia. J. Clin. Microbiol. 34, 2791–2794.

Kuboki, N., Inoue, N., Sakurai, T., Cello, F.Di., Grab, D.J., Suzuki, H., Sugimoto, C., Igarashi, I., 2003. Loop-mediated isothermal amplification for detection of African trypanosomes. J. Clin. Microbiol. 41, 5517–5524.

Massaro, W., Palmer, G.H., Kappmeyer, L.S., Scoles, G.A., Knowles, D.P., 2003. Expression of equi merozoite antigen 2 during development of *Babesia equi* in the midgut and salivary gland of the vector tick *Boophilus microplus*. J. Clin. Microbiol. 41, 5803–5809.

Melhorn, H., Schein, E., 1998. Redescription of *Babesia equi* Laveran, 1901 as *Theileria equi*. Parasitol. Res. 8, 467–475.

Mori, Y., Nagamine, K., Tomita, N., Notomi, T., 2001. Detection of loop-mediated isothermal amplification reaction by turbidity derived from magnesium pyrophosphate formation. Biochem. Biophys. Res. Commun. 289, 150–154.

Nicolaiewsky, T.B., Richter, M.F., Lunge, V.R., Cunha, C.W., Delagostin, O., Ikuta, N., Fonseca, A.S., da Silva, S.S., Ozaki, L.S., 2001. Detection of *Babesia equi* (Laveran 1901) by nested polymerase chain reaction. Vet. Parasitol. 101, 9–21.

Notomi, T., Hiroto, O., Harumi, M., Toshihiro, Y., Watanabe, K., Nobuyuki, A., Hase, T., 2000. Loop-mediated isothermal amplification of DNA. Nucleic Acids Res. 28, 63.

Schein, E., 1988. Equine babesiosis. In: Ristic, M. (Ed.), Babesiosis of Domestic Animals and Man. CRC Press, Boca Raton, FL, pp. 197–209.

Xu, Y., Zhang, S., Huang, X., Bayin, C., Xuan, X., Igarashi, I., Fujisaki, K., Kabeya, H., Maruyama, S., Mikami, T., 2003. Seroepidemiologic studies on *Babesia equi* and *Babesia caballi* infections in horses in Jilin Province of China. J. Vet. Med. Sci. 65, 1015–1017.

Xuan, X., Larsen, A., Ikadai, H., Tanaka, T., Igarashi, I., Nagasawa, H., Fujisaki, K., Toyoda, Y., Suzuki, N., Mikami, T., 2001. Expression of *Babesia equi* merozoite antigen 1 in insect cells by recombinant baculovirus and evaluation of its diagnostic potential in an enzyme-linked immunosorbent assay. J. Clin. Microbiol. 39, 705–709.

Effects of protein kinase inhibitors on the *in vitro* growth of *Babesia bovis*

S. BORK[1], S. DAS[1,2], K. OKUBO[1], N. YOKOYAMA[1] *and* I. IGARASHI[1]*

[1] *National Research Center for Protozoan Diseases, Obihiro University of Agriculture and Veterinary Medicine, Inada-cho, Obihiro, Hokkaido 080-8555, Japan*
[2] *Institute of Animal Health and Veterinary Biologicals, Animal Research Development Department, Kolkata, Government of West Bengal, India*

(*Received 8 August 2005; revised 1 December 2005; accepted 21 December 2005; first published online 24 February 2006*)

SUMMARY

Staurosporine, Ro-31-7549, and KN-93, which are inhibitors of serine/threonine protein kinase, protein kinase C, and calcium-modulin kinase, respectively, were tested for their effects on the *in vitro* growth of *Babesia bovis*. Staurosporine was the most effective inhibitor, completely clearing the parasitaemia as early as the first day of exposure at a concentration of 100 μM. Moreover, staurosporine caused a significant increase in the percentage of extracellular merozoites, most likely due to the inhibition of erythrocyte invasion by the parasite. Although 5 mM Ro-31-7549 and KN-93 had a suppressive action, this was not enough to destroy the parasite. Interestingly, concentrations of 0·5 to 5 mM KN-93 influenced the parasitic development within the infected erythrocytes. The present study suggests that *B. bovis* requires, to a certain extent, the phosphorylations mediated by parasite- or host erythrocyte-protein kinases, in particular, for the processes of successful invasion of erythrocytes and intraerythrocytic development.

Key words: staurosporine, Ro-31-7549, KN-93, *Babesia bovis*, *in vitro* cultivation.

INTRODUCTION

An intraerythrocytic protozoon, *Babesia bovis*, is one of the major causative agents of babesiosis in cattle (Sam-Yellowe, 1996; Homer *et al.* 2000). This parasite causes severe symptoms such as fever, anaemia, and cerebral dysfunctions during its erythrocytic stage, and thereby has a significant impact in the cattle industry worldwide (Kuttler, 1988). The host-parasite interaction between *B. bovis* and the host is complex. A better understanding of the biological processes involved in the growth cycle at the erythrocytic stage is required in order to develop effective therapeutic tools against bovine babesiosis (Bork *et al.* 2004*a*).

Protein kinases play essential roles in various signalling pathways of eukaryotic cells by catalysing the transfer of phosphate from ATP to an amino acid side-chain of a protein (Karin, 1991). They are vital for cell growth and survival (Bray, 1990). Any irregularity in their enzymatic activities may result in serious diseases, such as cancer, diabetes, and cardiovascular disorders (Komuro, 2001; Fulop, Larbi and Douziech, 2003; Russello and Shore, 2004). Since such protein phosphorylations are also essential in protozoa, notable advances have been made in determining the growth inhibitory activities of specific kinase inhibitors and clarifying the structure and function of the target protein kinases (Wiser and Schweiger, 1985; Flawia, Tellez-Inon and Torres, 1997; Doerig, 2004).

A serine/threonine kinase inhibitor, staurosporine (Becker and Jaffe, 1997), has broad biological activity ranging from anti-fungal (Sancelme, Fabre and Prudhomme, 1994) to anti-hypertensive (Berg, 2003). Additionally, it inhibits host cell invasion or growth of several *Plasmodium* species (Ward *et al.* 1994; Dluzewski and Garcia, 1996; Gazarini and Garcia, 2003), the epimastigotes of *Trypanosoma cruzi* (Vieira, de Carvalho and de Souza, 1994; Malaquias and Oliveira, 1999), and the promastigotes of *Leishmania major* and *L. amazonensis* (Becker and Jaffe, 1997). A selective protein kinase C (PKC) inhibitor, Ro-31-7549 (Hashimoto *et al.* 1997), is a potent down-regulator of several PKC-subtypes in human cancer cells (Turner *et al.* 1996), but study of its effect on protozoa is still lacking. Finally, a Ca^{2+}/calmodulin (CaM)-dependent protein (calcium-modulin) kinase inhibitor, KN-93 (Sumi *et al.* 1991), inhibited the growth of the epimastigotes of *T. cruzi* (Malaquias and Oliveira, 1999) and hampered the morphological development of the *P. gallinaceum* zygote to ookinete in mosquitoes (Silva-Neto, Atella and Shahabuddin, 2002). In the present work, we investigated the inhibitory activities of these protein kinase inhibitors on the growth of *B. bovis in vitro*.

* Corresponding author: National Research Center for Protozoan Diseases, Obihiro University of Agriculture and Veterinary Medicine, Inada-cho, Obihiro, Hokkaido 080-8555, Japan. Tel: +81 155 49 5641. Fax: +81 155 49 5643. E-mail: igarcpmi@obihiro.ac.jp

Parasitology (2006), **132**, 775–779.
doi:10.1017/S0031182006009917 Printed in the United Kingdom

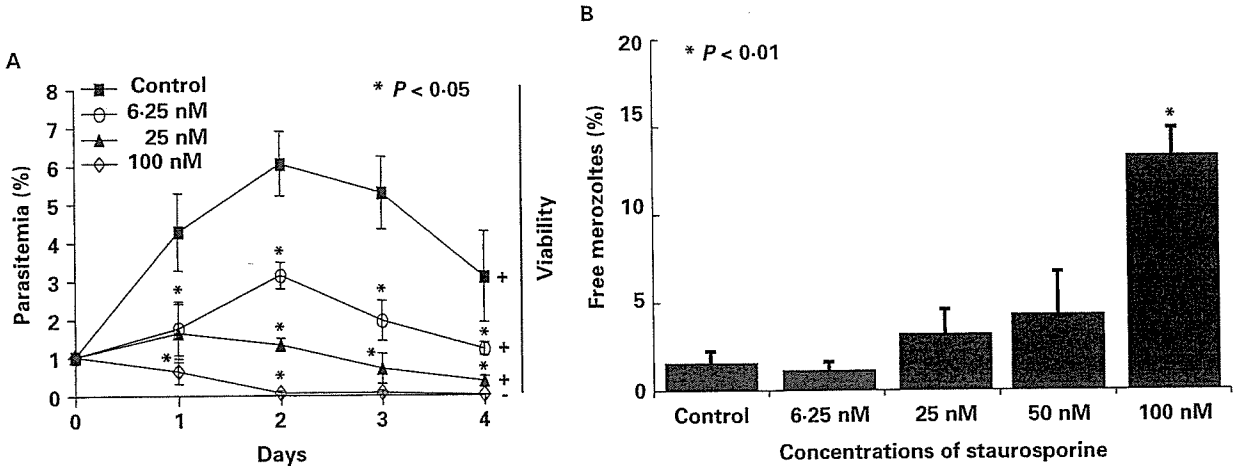

Fig. 1. (A) *In vitro* growth curves of *Babesia bovis* in the presence of different concentrations of staurosporine, based on the dynamics of parasitaemia. Parasitic viability: viable (+), dead (−). (B) Percentage of free merozoites in *in vitro* cultures of *B. bovis* exposed to different concentrations of staurosporine on the first day of culture. Each value represents the mean ± standard deviation (S.D.) in 3 separate trials carried out in triplicate. Asterisks indicate significant differences ($P<0{\cdot}05$ in (A) and $P<0{\cdot}01$ in (B)) between the drug-treated and control groups.

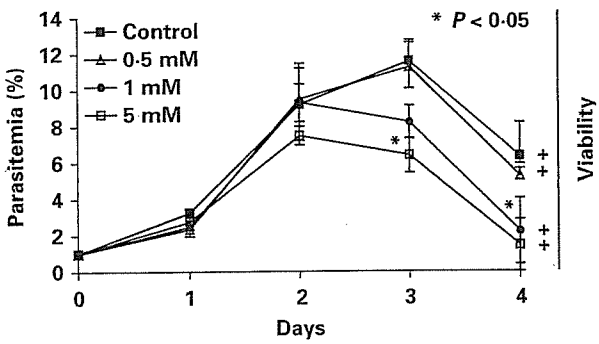

Fig. 2. *In vitro* growth curves of *Babesia bovis* in the presence of different concentrations of Ro-31-7549. Parasitic viability: viable (+), dead (−). Asterisks indicate significant differences ($P<0{\cdot}05$) between the drug-treated and control groups. Each value represents the mean ± S.D. in 3 separate trials conducted in triplicate.

MATERIALS AND METHODS

In vitro *cultivation of* B. bovis

The Texas strain of *B. bovis* was maintained in purified bovine erythrocytes in a serum-free GIT growth medium (Wako Pure Chemical Industrial Ltd., Osaka, Japan) as described previously (Bork *et al.* 2003*a*, 2004*b*, 2005).

Chemicals

Indolcarbazole staurosporine was purchased from Wako, and *bis*indolylmaleimide-VIII-acetate, Ro-31-7549, and the methoxybenzenesulfonamide KN-93 were obtained from Calbiochem (Darmstadt, Germany). Stock solutions of 1 M of the chemicals were prepared in dimethylsulfoxide (DMSO; Wako) and stored at −30 °C until use. Different drug concentrations were prepared by diluting the stock solution with the GIT medium. The concentrations of DMSO used in this study did not exert any abnormally inhibitory effects on the growth, as described previously (Bork *et al.* 2003*a*).

Growth inhibition assays

In vitro growth inhibition assays were performed as described previously (Bork *et al.* 2003*a*, *b*). In brief, 100 μl of infected bovine erythrocytes were diluted with non-infected erythrocytes to obtain 1% parasitaemia in a 0·1 ml volume, and the mixture was subsequently suspended in 0·9 ml of the growth medium supplemented with the indicated concentrations of chemicals. The suspension was added to 24-well culture plates (Nunk, Roskilde, Denmark), and the plates were incubated in a humidified multigas water-jacketed incubator at 37 °C for 4 days. During the incubation period, the overlaid culture medium was replaced daily with 0·9 ml of fresh growth medium containing the chemicals at the indicated concentrations. In parallel, chemical-free cultures were prepared as controls. Giemsa-stained thin blood smears were prepared daily, and the parasitic growth was monitored as parasitaemia by evaluating at least 1000 erythrocytes per well using light microscopy (Nikon, Tokyo, Japan). The percentage of extraerythrocytic (free) merozoites was calculated on the first day of culture as the ratio of free merozoites to the entire (intra- and extraerythrocytic) parasite population in approximately 250 parasites. The percentage of ring-shaped parasites was determined as the ratio of ring-shaped intraerythrocytic parasites to the entire amount of intraerythrocytic parasites in

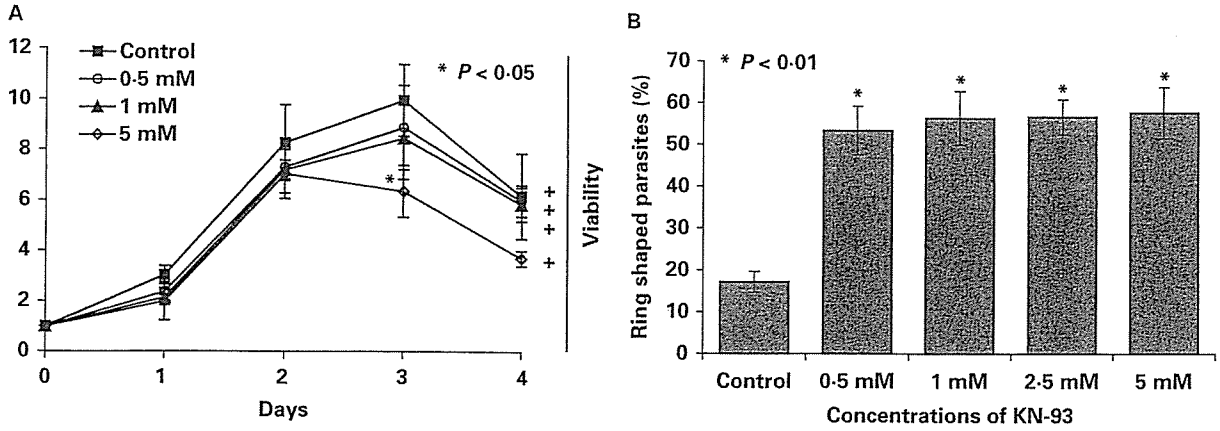

Fig. 3. (A) *In vitro* growth curves of *Babesia bovis* in the presence of different concentrations of KN-93. Parasitic viability: viable (+), dead (−). (B) Percentage of ring-shaped intraerythrocytic parasites in *in vitro* cultures of *B. bovis* exposed to different concentrations of KN-93 on the second day of culture. Each value represents the mean ± S.D. in 3 separate trials conducted in triplicate. Asterisks indicate significant differences ($P<0·05$ in (A) and $P<0·01$ in (B)) between the drug-treated and control groups.

approximately 250 parasites. Viability tests were also conducted following the method described by Bork *et al.* (2004*a*). In brief, after 4 days of chemical exposure, 30 μl of each of the infected and treated erythrocytes were mixed with 70 μl of non-infected erythrocytes and suspended in fresh growth medium without chemical supplementation. The plates were incubated for the next 10 days. The culture medium was replaced daily, and parasite recrudescence was determined by light microscopy to evaluate the parasite viability.

Statistical analysis

The 50% inhibition (IC_{50}) values of the drugs were determined in triplicate on the fourth day of *in vitro* culture after curve-fitting using Cricket Graph Software (Malvern, Pennsylvania, USA). Differences in the percentage parasitaemia and other percentages were statistically analysed using an independent Student's *t*-test at $P<0·01$ and $P<0·05$ as the values representing significant differences.

RESULTS

A concentration of 100 μM staurosporine irreversibly arrested the growth of *B. bovis* as early as the first day of *in vitro* culture, as shown in light microscopy and a subsequent viability test (Fig. 1A). During the time-course of the growth inhibition assay, concentrations from 6·25 to 50 μM significantly suppressed the parasitaemia but did not destroy the parasites. The IC_{50} value was determined as 5·12 μM. On the first day of culture, 25, 50, and 100 μM staurosporine resulted in substantial increases in the percentages of extraerythrocytic (free) merozoites, i.e. 3·2% ± 2·8, 4·8% ± 4·3, and 14·5% ± 4·1 ($P<0·01$), respectively, as compared to the non-treated control group (1·1% ± 1·1) (Fig. 1B). In the subsequent time-course with staurosporine, almost all of the free merozoites became pycnotic and died (data not shown).

Concentrations of 1 and 5 mM Ro-31-7549 reduced the parasitaemia, starting from the second and third day of culture, respectively. However, full destruction of the parasite was not observed and, additionally, a concentration below 1 mM did not exert any growth inhibitory effects on *B. bovis* (Fig. 2). The IC_{50} value was estimated as 4·83 mM.

Treatment with 5 mM KN-93 slightly but significantly hampered the parasitic growth as early as the third day of culture, but failed to completely clear the parasites from the culture (Fig. 3A). The IC_{50} value was estimated as 11·75 mM. Interestingly, on the second day of culture, the percentages of ring-shaped parasites within the infected erythrocytes increased ($P<0·01$) in the cultures treated with 0·5 mM (53·3% ± 5·8), 1 mM (56·3% ± 6·4), 2·5 mM (56·7% ± 4·2), and 5 mM (57·7% ± 6·1) of KN-93, as compared to the control (17·1% ± 2·5) (Fig. 3B).

DISCUSSION

In this study, 3 kinds of protein kinase inhibitors were shown to have substantial inhibitory effects on the *in vitro* growth of *B. bovis*. Among them, the serine/threonine kinase inhibitor, staurosporine, showed the strongest activity of growth inhibition. The significant increase in the percentage of free merozoites in the staurosporine-treated cultures might be attributed to the inhibition of the parasite's invasion into host erythrocytes. Our findings correspond to previous publications reporting that staurosporine significantly inhibited the erythrocyte invasions by *P. knowlesi* (Ward *et al.* 1994), *P. falciparum* (Dluzewski and Garcia, 1996), and *P. chabaudi* (Gazarini and Garcia, 2003) in their cultures. The inhibitory mechanism, however,

remains unclear yet, because the significant increase of free merozoites was accomplished only at the highest concentration of staurosporine that affected the parasite viability in this study. Further study will be required to understand the inhibitory mechanism of staurosporine on *B. bovis*.

The PKC-inhibitor, Ro-31-7549, has not been studied in any protozoa. Thus, our work is the first study of its possible inhibitory effect on the propagation of *B. bovis*. Previously, Ray *et al.* (1990) demonstrated that *B. bovis* possesses a powerful PKC activity in the parasitic membrane. However, the growth inhibition activity of Ro-31-7549 was not as high as we initially expected. Whether the result in our growth inhibition assay was due to insufficient drug concentrations used in our study or the possibilities that Ro-31-7549 may not be a specific inhibitor of PKC activity in *B. bovis* or that PKC activity may not be essential for *in vitro* growth, remains to be elucidated.

Although treatment with a Ca^{2+}/CaM-dependent protein kinase inhibitor, KN-93, failed to effectively interrupt the parasitic propagation, it caused a significant increase in the percentage of ring-shaped parasites, which are the early forms after erythrocyte invasion that follow the subsequent division to 2 elongated parasites (Levine, 1988). This morphological phenomenon was also observed in the *Plasmodium* species (Silva-Neto *et al.* 2002). Ray *et al.* (1990) demonstrated the existence of a Ca^{2+}/CaM environment in *B. bovis* and mentioned a possible correlation between the growth of *B. bovis* and Ca^{2+}-dependent protein phosphorylation by kinases. For understanding the biological effect of KN-93 on *B. bovis*, it is necessary to identify the Ca^{2+}/CaM-dependent protein kinase of *B. bovis* and investigate its relationship with the morphological shape changes from ring-shaped to elongated *Babesia* parasites.

Our endeavour to work with these protein kinase inhibitors will contribute to the understanding of the biological mechanisms of erythrocyte invasion and development of *B. bovis* in future. In particular, the identification of the target protein kinases, which possibly exist in the parasite or host erythrocyte, is of major interest. A more detailed exploration of the biological roles of protein kinases involved in the asexual growth of *Babesia* parasites will pave the way for a better understanding and control of bovine babesiosis.

This work was supported by Grants-in-Aid for Scientific Research from the Japanese Society for the Promotion of Science, by grants from the Special Coordination Funds for Science and Technology from the Science and Technology Agency and from The 21st Century COE Program (A-1), Ministry of Education, Culture, Sports, Science, and Technology, Japan, and by the Japan International Cooperation Agency (JICA), F.Y. 2003.

REFERENCES

Becker, S. and Jaffe, C. L. (1997). Effect of protein kinase inhibitors on the growth, morphology, and infectivity of *Leishmania* promastigotes. *Parasitology Research* **83**, 273–280.

Berg, T. (2003). The vascular response to the K+ channel inhibitor 4-aminopyridine in hypertensive rats. *European Journal of Pharmacology* **466**, 301–310.

Bork, S., Yokoyama, N., Matsuo, T., Claveria, F. G., Fujisaki, K. and Igarashi, I. (2003*a*). Growth inhibitory effect of triclosan on equine and bovine *Babesia* parasites. *American Journal of Tropical Medicine and Hygiene* **68**, 334–340.

Bork, S., Yokoyama, N., Matsuo, T., Claveria, F. G., Fujisaki, K. and igarashi, I. (2003*b*). Clotrimazole, ketoconazole, and clodinafop-propargyl as potent growth inhibitors of equine *Babesia* parasites during *in vitro* culture. *Journal of Parasitology* **89**, 604–606.

Bork, S., Yokoyama, N., Ikehara, Y., Kumar, S., Sugimoto, C. and Igarashi, I. (2004*a*). Growth inhibitory effect of heparin on *Babesia* parasites. *Antimicrobial Agents and Chemotherapy* **48**, 236–241.

Bork, S., Okamura, M., Boonchit, S., Hirata, H., Yokoyama, N. and Igarashi, I. (2004*b*). Identification of *Babesia bovis* L-lactate dehydrogenase as a chemotherapeutical target against bovine babesiosis. *Molecular and Biochemical Parasitology* **136**, 165–172.

Bork, S., Okamura, M., Matsuo, T., Kumar, S., Yokoyama, N. and Igarashi, I. (2005). Host serum modifies the drug susceptibility of *Babesia bovis in vitro*. *Parasitology* **130**, 489–492.

Bray, D. (1990). Intracellular signaling as a parallel distributed process. *Journal of Theoretical Biology* **143**, 215–231.

Dluzewski, A. R. and Garcia, C. R. (1996). Inhibition of invasion and intraerythrocytic development of *Plasmodium falciparum* by kinase inhibitors. *Experientia* **52**, 621–623.

Doerig, C. (2004). Protein kinases as targets for anti-parasitic chemotherapy. *Biochimica et Biophysica Acta* **1697**, 155–168.

Flawia, M. M., Tellez-Inon, M. T. and Torres, H. N. (1997). Signal transduction mechanisms in *Trypanosoma cruzi*. *Parasitology Today* **13**, 30–33.

Fulop, T., Larbi, A. and Douziech, N. (2003). Insulin receptor and ageing. *Pathologie-biologie* **51**, 574–580.

Gazarini, M. L. and Garcia, C. R. (2003). Interruption of the blood-stage cycle of the malaria parasite, *Plasmodium chabaudi*, by protein tyrosine kinase inhibitors. *Brazilian Journal of Medical and Biological Research* **36**, 1465–1469.

Hashimoto, Y., Togo, M., Sato, H., Hashimoto, N., Watanabe, T., Kurokawa, K. and Nakahara, K. (1997). Characteristics of protein kinase C-independent exocytosis in human platelets. *Thrombosis Research* **88**, 51–58.

Homer, M. J., Aguilar-Delfin, I., Telford, S. R. 3rd, Krause, P. J. and Persing, D. H. (2000). Babesiosis. *Clinical Microbiology Review* **3**, 451–469.

Karin, M. (1991). Signal transduction and gene control. *Current Opinion in Cell Biology* **3**, 467–473.

Komuro, I. (2001). Molecular mechanism of cardiac hypertrophy and development. *Japanese Circulation Journal* **655**, 353–358.

Kuttler, K. L. (1988). Worldwide impact of babesiosis. In *Babesiosis of Domestic Animals and Man* (ed. Ristic, M.), pp. 2–22. CRC Press Inc., Boca Raton, Florida, USA.

Levine, N. D. (1988). *The Protozoan Phylum Apicomplexa. Vol. 2.* CRC Press, Boca Raton, Florida, USA.

Malaquias, A. T. and Oliveira, M. M. (1999). Phospholipid signaling pathways in *Trypanosoma cruzi* growth control. *Acta Tropica* **73**, 93–108.

Ray, A., Quade, J., Carson, C. A. and Ray, B. K. (1990). Calcium-dependent protein phosphorylation in *Babesia bovis* and its role in growth regulation. *Journal of Parasitology* **76**, 153–161.

Russello, S. V. and Shore, S. K. (2004). SRC in human carcinogenesis. *Frontiers in Bioscience* **9**, 139–144.

Sam-Yellowe, T. Y. (1996). Rhoptry organelles of the apicomplexa: their role in host cell invasion and intracellular survival. *Parasitology Today* **12**, 308–316.

Sancelme, M., Fabre, S. and Prudhomme, M. (1994). Antimicrobial activities of indolocarbazole and bis-indole protein kinase C inhibitors. *Journal of Antibiotics* **47**, 792–798.

Silva-Neto, M. A., Atella, G. C. and Shahabuddin, M. (2002). Inhibition of Ca2+/calmodulin-dependent protein kinase blocks morphological differentiation of *Plasmodium gallinaceum* zygotes to ookinetes. *Journal of Biological Chemistry* **277**, 14085–14091.

Sumi, M., Kiuchi, K., Ishikawa, T., Ishii, A., Hagiwara, M., Nagatsu, T. and Hidaka, H. (1991). The newly synthesized selective Ca2+/calmodulin-dependent protein kinase II inhibitor KN-93 reduces dopamine contents in PC12h cells. *Biochemical and Biophysical Research Communications* **181**, 968–975.

Turner, N. A., Walker, J. H., Ball, S. G. and Vaughan, P. F. (1996). Down-regulation or long-term inhibition of protein kinase C (PKC) reduces noradrenaline release evoked via either PKC-dependent or PKC-independent pathways in human SH-SY5Y neuroblastoma cells. *Neuroscience Letters* **220**, 37–40.

Vieira, M. C., De Carvalho, T. U. and De Souza, W. (1994). Effect of protein kinase inhibitors on the invasion process of macrophages by *Trypanosoma cruzi*. *Biochemical and Biophysical Research Communications* **203**, 967–971.

Ward, G. E., Fujioka, H., Aikawa, M. and Miller, L. H. (1994). Staurosporine inhibits invasion of erythrocytes by malarial merozoites. *Experimental Parasitology* **79**, 480–487.

Wiser, M. F. and Schweiger, H. G. (1985). Cytosolic protein kinase activity associated with the maturation of the malaria parasite *Plasmodium berghei*. *Molecular and Biochemical Parasitology* **17**, 179–189.

Available online at www.sciencedirect.com
SCIENCE DIRECT
ELSEVIER
Molecular & Biochemical Parasitology 145 (2006) 171–183
MOLECULAR & BIOCHEMICAL PARASITOLOGY

Kinetics and strain variation of phagosome proteins of *Entamoeba histolytica* by proteomic analysis

Mami Okada[a,b,c,1], Christopher D. Huston[d,2], Miho Oue[a,1], Barbara J. Mann[e,3], William A. Petri Jr.[f,4], Kiyoshi Kita[b,5], Tomoyoshi Nozaki[a,c,*]

[a] *Department of Parasitology, Gunma University Graduate School of Medicine, 3-39-22 Showa-machi, Maebashi, Gunma 371-8511, Japan*
[b] *Department of Biomedical Chemistry, Graduate School of Medicine, The University of Tokyo, 7-3-1 Hongo, Bunkyo, Tokyo 113-0033, Japan*
[c] *The Precursory Research for Embryonic Science and Technology, Japan Science and Technology Agency, 2-20-5 Akebono-cho, Tachikawa, Tokyo 190-0012, Japan*
[d] *Department of Medicine, University of Vermont College of Medicine, 95 Carrigan Drive, Burlington, VT 05405, USA*
[e] *Departments of Internal Medicine and Microbiology, University of Virginia Health System, Charlottesville, VA 22908-1340, USA*
[f] *Department of Medicine, Microbiology, and Pathology, University of Virginia Health System, Charlottesville, VA 22908-1340, USA*

Received 25 August 2005; received in revised form 29 September 2005; accepted 3 October 2005
Available online 19 October 2005

Abstract

The protozoan parasite *Entamoeba histolytica* ingests and feeds on microorganisms and mammalian cells. Phagocytosis is essential for cell growth and implicated in pathogenesis of *E. histolytica*. We report here the dynamic changes of phagosome proteins during phagosome maturation by proteomic analysis using reversed-phase capillary liquid chromatography and ion trap tandem mass spectrometry. Phagosomes were isolated at various intervals after internalization of latex beads. Immunoblot analysis and electron microscopy verified successful isolation of phagosomes. A total of 159 proteins were identified from the reference strain HM1 at different stages of phagosome maturation. Approximately 70% of them were detected in a time-dependent fashion, suggesting dynamism of phagosome biogenesis. The kinetics of representative proteins were verified by immunoblots and also by video microscopy of live transgenic amebae expressing green fluorescent protein-fused EhRab7A. Furthermore, we observed significant differences in phagosome profiles between HM1 and two recent clinical isolates. Approximately 60% of 229 proteins detected in at least one of these three strains were identified only in one strain, while approximately 20% of these proteins were detected in all three strains. These data should provide significant insights into molecular characterization of phagosome biogenesis, and help to elucidate the pathogenesis of this important infection.

Keywords: Amebiasis; Protist; Phagocytosis; Proteome; Pathogenesis

1. Introduction

The protozoan parasite *Entamoeba histolytica* is an anaerobic or microaerophilic eukaryote, which is a major cause of morbidity and mortality worldwide [1]. *E. histolytica* colonizes the large intestine, causing amebic dysentery and is occasionally disseminated to other organs (e.g., liver, lung, and brain), resulting in often lethal abscesses. There are an estimated 10 million cases of amebiasis annually [2]. *E. histolytica* is capable of internalizing extracellular substances by pinocytosis, macropinocytosis, and phagocytosis [3]. The amebic trophozoites ingest microorganisms in the large intestine [4], and host cells including non-immune cells [5], and immune cells [6] during tissue invasion. It has been well-established that phagocytosis plays an essential role in growth and also constitutes one of the key virulence determinants [7]. Downregulation of calcium-binding protein 1 by antisense resulted in inhibition of both cellular proliferation and phagocytosis [8]. In addition, ameba mutants defective in

Abbreviations: CP, cysteine protease; GFP, green fluorescent protein; Hgl, Gal/GalNAc-specific lectin heavy subunit; Igl, Gal/GalNAc-specific lectin intermediate subunit; Lgl, Gal/GalNAc-specific lectin light subunit

* Corresponding author. Tel.: +81 27 220 8020; fax: +81 27 220 8025.
E-mail address: nozaki@med.gunma-u.ac.jp (T. Nozaki).
[1] Tel.: +81 27 220 8024; fax: +81 27 220 8025.
[2] Tel.: +1 802 656 9115; fax: +1 802 847 5322.
[3] Tel.: +1 434 924 9666; fax: +1 434 924 0075.
[4] Tel.: +1 434 924 5621; fax: +1 434 924 0075.
[5] Tel.: +81 3 5841 3526; fax: +81 3 5841 3444.

0166-6851/$ – see front matter © 2005 Elsevier B.V. All rights reserved.
doi:10.1016/j.molbiopara.2005.10.001

phagocytosis were also defective in the destruction of tissue-cultured mammalian cells in vitro and in the formation of hepatic abscesses in vivo [9]. Therefore, understanding molecular mechanisms of phagocytosis should help in the identification of underlying links between phagocytosis and proliferation, and between phagocytosis and pathogenicity, which might help to develop novel measures to control amebiasis.

Recent advances in proteomic analysis have made it possible to identify proteins involved in particular biological processes of interest with high throughput and wide dynamic range. A global overview of the amebic phagosome demonstrated by our previous proteomic analysis enabled us to identify a group of novel proteins involved in phagosome biogenesis [10]. We reported that 85 phagosome proteins involved in surface recognition, cytoskeleton, vesicular trafficking, and degradation were detected in primary phagosomes isolated within 5 min of internalization. However, the kinetics of phagosome proteins during maturation and biogenesis of phagosomes remain totally uncharacterized. In the present study, the changing protein profiles of isolated phagosomes at time points during phagosome maturation were determined by proteomic analysis. Our analysis demonstrates a striking dynamism of phagosome-associated proteins. The kinetics of representative phagosome proteins are validated by immunoblots and by video microscopy using live ameba expressing a green fluorescent protein (GFP)-fused phagosome protein. Furthermore, we demonstrate a significant variation of the phagosome proteins among *E. histolytica* strains [11] by comparing the protein profiles from HM-1:IMSS cl 6 reference strain and two recent clinical isolates.

2. Materials and methods

2.1. Microorganisms and cultivation

E. histolytica trophozoites of a clonal strain HM-1:IMSS cl 6 (HM1) [12] and two recent clinical isolates (KU33, isolated from an amebic dysentery patient in Kanagawa, Japan [11], and HATAJI, isolated from an amebic dysentery patient in November 1992 in Osaka, Japan) were analyzed in this study. HM1 trophozoites were axenically cultivated in BI-S-33 medium at 37 °C as described previously [12]. HATAJI and KU33 were monoxenically cultivated in BI-S-33 medium with *Crithidia fasciculata* at 37 °C [13]. The amebic trophozoites were routinely cultivated in 25 cm^2 flasks (NUNC, Roskilde, Denmark) and regularly passaged before the cultures reached the late-logarithmic growth phase.

2.2. Antibodies

Mouse monoclonal antibodies against Gal/GalNAc-specific lectin heavy subunit (Hgl) (3F4 [14]), intermediate subunit (Igl) [15], and light subunit (Lgl) (1C8 and 3C2 [16]) have been previously described. Rabbit polyclonal antibodies against cysteine synthase 1 [17], methionine γ-lyase 1 and 2 [18], nitrogen fixation S and U [19], and alcohol dehydrogenase 1 [20] were previously described. Polyclonal rabbit antibodies were commercially raised against histidine-tagged *Escherichia coli* recombinant proteins of cysteine protease 5 (CP5), dipeptidyl aminopeptidase, Rab7A, Rab7E, and Rab11B. Rabbit antibody against cysteine protease 1 (CP1) was a generous gift from Sharon L. Reed, UCSF, USA. Horseradish peroxidase-conjugated goat anti-mouse or anti-rabbit IgGs were purchased from Molecular Probes.

2.3. Isolation, and purification of phagosomes

The trophozoites were cultured in 25 cm^2 flasks for 48 h (from 3×10^6 to 5×10^6 per flask), and washed gently with warm Opti-MEM (Invitrogen, Tokyo, Japan) supplemented with 1 mg/ml ascorbic acid and 5 mg/ml cysteine. After 10^7 carboxylate-modified latex beads (Sigma, St. Louis, MO) were added to the flasks, they were centrifuged at $160 \times g$ for 5 min to bring the beads into contact with the trophozoites. After centrifugation, phagosome maturation was immediately interrupted by incubating the flasks on ice for 10 min, followed by washing once with cold PBS. The trophozoites were washed three additional times with cold PBS containing 20% sucrose, followed by centrifugation to remove uningested beads. The resulting cell pellet was virtually free from unincorporated beads (data not shown). The cells containing latex beads were then resuspended in warm BI-S-33 medium, further incubated at 37 °C, and harvested after 30, 60, and 120 min.

Bead-containing phagosomes were purified as previously described [10] with some modifications. Briefly, after harvesting, the amebae-containing latex beads were resuspended in cold homogenization buffer (250 mM sucrose, pH 7.4, 3 mM imidazole, 10 mM cysteine protease inhibitor E-64, Complete Mini protease inhibitor cocktail) and homogenized on ice in a Dounce homogenizer. Phagosomes containing latex beads were then separated by flotation on a sucrose step gradient as described [10]. All sucrose solutions were made in 3 mM imidazole, pH 7.4 containing 10 mM cysteine protease inhibitor E-64. Sucrose was added to the homogenized lysate to 40%. 2 ml of the lysate containing 40% sucrose, 2 ml each of 35, 25, and 10% sucrose solutions were carefully overlaid in a 10 ml ultracentrifuge tube. The sample was centrifuged in a swinging bucket rotor SW40 (Beckman, Tokyo, Japan) at $100,000 \times g$ at 4 °C for 1 h. The phagosome fraction was collected from the interface of the 10 and 25% sucrose solutions. The collected 1 ml fraction was mixed with 3 ml of 50% sucrose, and transferred to a new tube. To the sample, 4 ml of 25% and 2 ml of 10% sucrose solutions were overlaid, and the sample was centrifuged at $100,000 \times g$ at 4 °C for 1 h. The separated phagosome sample, collected from the interface of the 10 and 25% sucrose solutions, was finally mixed with the same volume of 3 mM imidazole solution and centrifuged at $13,000 \times g$ at 4 °C for 5 min. At least two independent phagosome samples were prepared for each time point.

2.4. Protein digestion, LC–MS, and MS/MS

Phagosome peptide analysis was carried out at the W.M. Keck Biomedical Mass Spectrometry Laboratory at the University of Virginia. Briefly, the solution samples were transferred

to a siliconized tube, dehydrated in acetonitrile, rehydrated in 30 μl of 10 mM dithiothreitol in 0.1 M ammonium bicarbonate and reduced at room temperature for 30 min. The sample was then alkylated in 30 μl of 50 mM iodoacetamide in 0.1 M ammonomium bicarbonate at room temperature for 30 min. The reagent was removed and the sample was dehydrated in 100 μl acetonitrile, rehydrated in 100 μl of 0.1 M ammonium bicarbonate, and then dehydrated again in 100 μl acetonitrile and completely dried by vacuum centrifugation. Samples were then rehydrated in 20 ng/ml trypsin in 50 mM ammonium bicarbonate on ice for 10 min. Any excess trypsin solution was removed and 20 μl of 50 mM bicarbonate added. The samples were digested overnight at 37 °C and resultant peptides were extracted in two 30 μl aliquots of 50% acetonitrile/5% formic acid. These extracts were combined and evaporated to 25 μl for MS analysis.

The LC–MS system consisted of a Finnigan LCQ ion trap mass spectrometer system with a Protana nanospray ion source interfaced to a self-packed 8 cm × 75 μm i.d. Phenomenex Jupiter 10 μm C18 reversed-phase capillary column. The volumes of the extract (0.5–5 μl) were injected and the peptides eluted from the column by an acetonitrile/0.1 M acetic acid gradient at a flow rate of 0.25 μl/min. The nanospray ion source was operated at 2.8 kV. The digest was analyzed using the double play capability of the instrument acquiring full scan mass spectra to determine peptide molecular weights and product ion spectra to determine amino acid sequence in sequential scans. This mode of analysis produces approximately 400 CAD spectra of ions ranging in abundance over several orders of magnitude.

2.5. Database search

Peptide sequence data were analyzed versus The Institute for Genomic Research (TIGR) *E. histolytica* genome database (http://www.tigr.org/tdb/e2k1/eha1/) [21] using the Sequest algorithm [22]. Sequencing data were also analyzed against the non-redundant database at the National Center of Biotechnology Information (NCBI). Individual predicted protein sequences were then manually analyzed by BLAST search (http://www.ncbi.nlm.nih.gov/BLAST/) against the non-redundant database at NCBI. The identification of the protein was considered significant when there were at least two non-overlapping peptides of a protein detected. The identified proteins were classified using the annotations provided in the TIGR and NCBI database and results of BLAST search.

2.6. Electron microscopy

Crude homogenates derived from the amebae that had ingested carboxylate-modified latex beads and purified phagosomes were examined by electron microscopy to verify purity and integrity of the isolated phagosomes. The samples were fixed with 2.5% glutaraldehyde–2% paraformaldehyde in 0.1 M phosphate buffer (pH 7.4) for 1 h at 4 °C, then post-fixed with 1% osmium tetroxide in the same buffer for 1 h at 4 °C. The fixed specimens were solidified with 2% agarose, followed by dehydration in a graded series of ethanol, and embedded in Epon 812 (TAAB Laboratories Equipment Ltd., Berkshire, UK). Ultrathin sections were made on an LKB-ultramicrotome (LKB-Pruodukter, Bromma, Sweden). After staining with uranyl acetate and lead citrate, the specimens were examined with a JEOL JEM-1010 electron microscope (Peabody, MA).

2.7. Immunoblot analysis

The purity of phagosome and the relative amount of phagosome proteins were evaluated by immunoblot analysis, carried out as described previously [23]. Blots were reacted with primary antibodies at a dilution of 1:100–1:500. After the blots were further reacted with horseradish peroxidase-conjugated anti-mouse or rabbit IgG antisera (1:1000), specific proteins were visualized with chemiluminescent substrate (Pierce, Rockford, IL) according to the manufacturer's protocol. The relative amount of each protein was measured on Fluor-S MAX2 Multi Imager with Quantity one Version 4.02 (Bio-Rad, Tokyo, Japan). The total amount of proteins of individual samples was normalized with SYPRO Ruby (Bio-Rad) staining of the protein gels.

2.8. Video microscopy

Recruitment and dissociation of phagosome proteins were monitored using a transformant ameba line expressing a representative phagosome protein *Eh*Rab7A [24] fused with GFP (GFP-*Eh*Rab7A) on video microscopy. Approximately, 10^4 GFP-*Eh*Rab7A-expressing transformants [24] were seeded on a 0.79 cm^2 well of a collagen-coated glass bottom culture dish (MatTek Corporation, Roskilde, Denmark) and mixed with 10^4 blue fluorescent calboxylate-modified beads (Molecular Probes). After the mixture was enclosed with a cover slip, it was further incubated at 33 °C in a temperature control unit on AS Multi Dimension Workstation (Leica Microsystems, Wetzlar, Germany). Sequential images of trophozoites that ingested a single bead were captured every 1 min for 2 h on a DM IRE2 inverted microscope with a HC PLAN APO 63x objective (Leica) integrated in Leica AS Multi Dimension Workstation system. GFP and blue fluorescence images of 100 continuous slices (z-stack) with 0.3 μm intervals were acquired with a Roper Cool Snap HQ digital camera (Roper Scientific Inc., Duluth, GA) at excitation wavelength of 467 and 393 nm with BGR filter (#11,513,838). The images were processed with a non-blind deconvolution algorithm using the "Deblur" module provided with the AS Multi Dimension Workstation system.

3. Results and discussion

3.1. Purity of the phagosome preparations

The purity of the isolated phagosomes was verified by two independent methods. First, transmission electron micrographs of the phagosome preparations showed that the bead-associated fraction was enriched in phagosomes (Fig. 1A-a), while the cell lysate of the trophozoites contained a large number of granular, vesicular, and vacuolar structures varying in size and shape (Fig. 1A-b). The membrane integrity of approximately 90% of

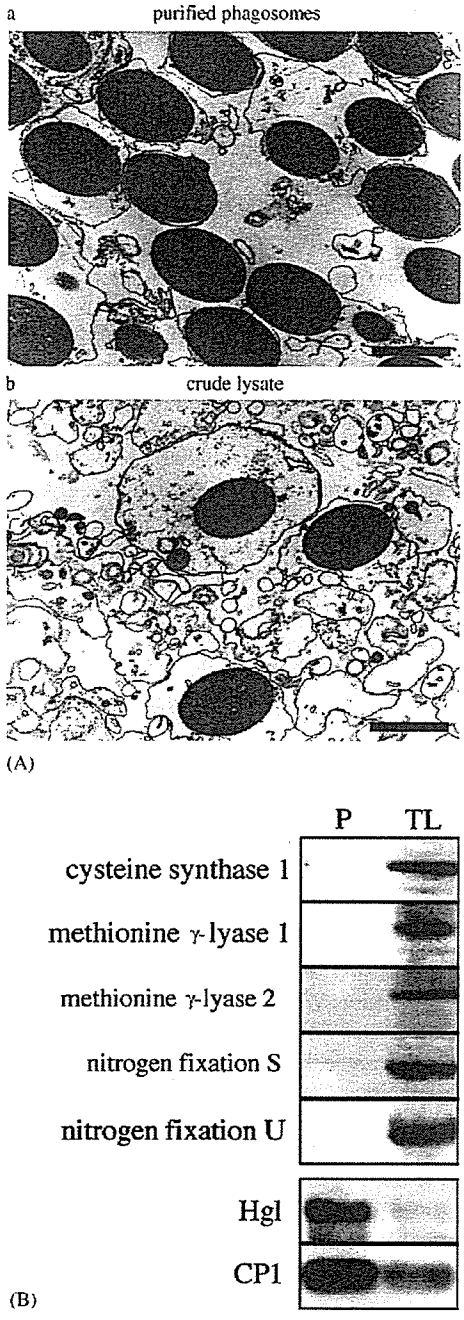

Fig. 1. Purity of the isolated phagosomes. (A) Transmission electron micrographs of: (a) the phagosome-enriched fraction after sucrose step gradient centrifugation (purified phagosomes) and (b) the ameba crude homogenate (bar = 2 μm) (crude lysate). (B) Immunoblot analysis of the isolated phagosomes. Approximately, 10 μg each of the isolated phagosome (P) and total crude lysate (TL) were separated by SDS-polyacrylamide electrophoresis, blotted onto a nitrocellulose membrane, and reacted with antibodies against cytosolic proteins cysteine synthase 1, methionine γ-lyase 1 and 2, and nitrogen fixation S and U and against phagosome proteins Hgl and CP1.

the isolated phagosomes was preserved. Second, immunoblot analysis showed that the phagosome preparations were devoid of known cytosolic proteins (Fig. 1B). Specific polyclonal antibodies against cysteine synthase 1, methionine γ-lyase 1 and 2, nitrogen fixation S and U, and alcohol dehydrogenase 1 (data not shown) did not react with the phagosome preparations, but did recognize proteins of the predicted molecular mass in total cell lysate. In contrast, Hg1 and hydrolytic enzyme CP1 were enriched in the purified phagosomes compared to total cell lysate, which is consistent with our previous identification of these proteins in the purified phagosomes [10].

3.2. Overall proteomic profiles of the purified phagosomes

We examined protein profiles of the purified phagosomes isolated at different stages of maturation. We analyzed trypsin-digested fragments derived from the purified phagosomes using reversed-phase capillary liquid chromatography and ion trap tandem mass spectrometry. Peptide sequences of a total of 6043 peptides (600–1100 peptides per sample) that were obtained from four time points with biological duplicate samples of each time point, were determined in the HM1 reference strain, and unequivocally assigned to 159 proteins with the sequence coverage of 3–70%. An overview of these proteins identified at different intervals (0, 30, 60, and 120 min after internalization of beads) is shown in Fig. 2A. The profiles of phagosomes obtained at 30 and 60 min were combined for clarity, as they were the closest pair among the four time points (data not shown). When the proteins were compared among early (0 min), intermediate (30 and 60 min), and late phases of phagosome maturation (120 min), 68% of proteins was detected at one or two phases, while only 32% of proteins were constitutively detected. Since contamination would be unaffected by the chase time, this further supports the purity of the phagosome preparations and is consistent with a dynamic recruitment and dissociation of numerous proteins during phagosome maturation. Table 1 shows 103 phagosome proteins, out of a total of 159 proteins detected in our analysis that have known or predicted functions in *E. histolytica* or possess higher than 25% amino acid identity and an *E*-value of lower than 10^{-5} compared to proteins from other organisms. The remaining 56 proteins were "hypothetical proteins" and not listed (Supplementary Table SI). These 103 proteins were categorized as vesicular trafficking proteins (16%), hydrolytic enzymes (14%), cytoskeletal proteins (6%), signal transduction (5%), lectins and surface proteins (5%), calcium and proton pumps (3%), mitochondria-like proteins (2%), and other proteins (15%). It is worth noting that hypothetical proteins without predictable functions accounted for the largest proportion of phagosome proteins (34%), suggesting that these unique hypothetical proteins might provide new insights into molecular mechanisms of phagosome biogenesis.

3.3. Kinetic profiles of the representative phagosome proteins

Kinetic profiles of phagosome proteins were categorized into several classes including constitutive, early-, intermediate-, and late-phase recruitment as well as biphasic recruitment at early and late phases with intermittent dissociation between these two phases. For instance, some proteins involved in vesicular trafficking, such as Rab1, Rab5, Rab7D, RabC1, and receptor-

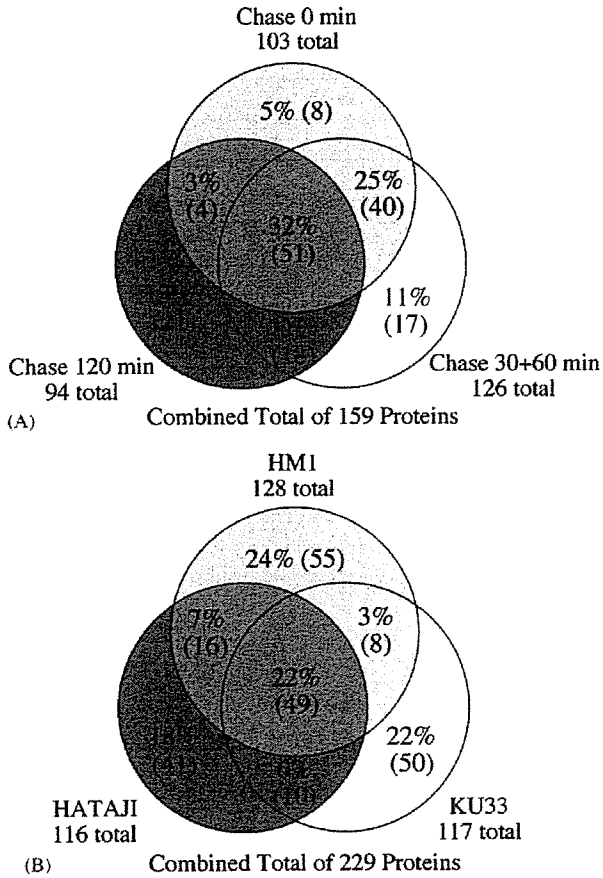

Fig. 2. Diagram showing an overview of phagosome proteins. (A) The profiles of phagosomes isolated at early, intermediate, and late phases of phagosome maturation were compared. Note that proteins detected at 30 and 60 min after the bead internalization were combined. (B) The profiles of phagosomes isolated from HM1, KU33, and HATAJI were compared. Note that individual profiles contain proteins detected at 0 or 30 min, or both.

mediated endocytosis protein 1 homologue, were present at 0 and 60 min, but absent at 30 min. We previously showed that Rab5 is involved in engulfment of erythrocytes and the transport of lysosomal hydrolases to phagosomes through a compartment uniquely identified in this organism [24]. The presence of Rab5 in bead-containing phagosomes, together with the lack of Rab5 in erythrocyte-containing phagosomes in our previous study, suggests that the recruitment of Rab5 to phagosomes may depend on ingested materials. Rab7 isotypes showed isotype-specific and time-dependent recruitment to phagosomes. Among nine Rab7 isotypes present in the genome [25], five isotypes were identified. Both Rab7B and 7C were detected in the early to intermediate phase (0–60 and 0–30 min, respectively), while Rab7A and 7E showed a constitutive phagosome association. On the other hand, Rab7D showed biphasic recruitment (0 and 60 min). These data suggest an elaborate regulation of association and dissociation of Rab7 isotypes to phagosomes. Since these Rab7 isotypes share effector proteins, as predicted from the high homology in the effector-binding region [25], and thus, are presumably regulated by common effectors, additional mechanisms to determine isotype-specific recruitment to phagosomes appear likely. None of components of the retromer-like complex, which was previously shown to be a novel Rab7A effector that transports cysteine proteases in *E. histolytica* [26], was found in our proteomic analysis, suggesting the interaction between the complex and EhRab7A is either transient or unstable.

Most of identified hydrolytic enzymes (81%) were detected at the early phase of phagosome biogenesis (0 min) and present in all time points, indicating that lysosomal hydrolases were acquired rapidly after the phagosome formation and continuously associated with phagosomes in *E. histolytica*. This result is consistent with our recent finding that phagosomes-containing internalized yeasts were rapidly acidified within 2 min after the phagosome formation and the phagosome acidity remained constant for over 12 h in *E. histolytica* [27]. These data are similar to the observations in the other organisms including human and rat leukocytes, and *D. discoideum*, where the acidification of phagosomes and the recruitment of lysosomal enzymes occurred within 3–15 min after ingestion [28–30]. Similar to the vesicular transporting proteins including Rabl and Rab7D, a number of hydrolytic enzymes including β-amylase, acid phosphatase, some phosphatases, and surface protease had two peaks of recruitment at 0 and 60 min, raising the possibility that these hydrolases and Rab proteins may be co-transported to phagosomes. A similar biphasic pattern of association and dissociation was also observed for various other proteins including cytoskeletal proteins and a calcium pump. The biphasic recruitment was previously reported for phosphatidylinositol-3-phosphate in macrophages. It was shown that phosphatidylinositol-3-phosphate was recruited to phagosomes in temporally organized cyclical waves, with the average periodicity of 20 min, in the course of phagosome maturation [31]. These two waves were shown to be regulated by two independent mechanisms, since the second wave was calmodulin-dependent and inhibited by *Mycobacterium* infection, while the first was not. It was also shown that actin assembly and disassembly repeatedly occurred on the phagosome membrane of MDCK epithelial cells that were infected by *Listeria monocytogenes* or *E. coli* that expressed invasin from *Yersinia pseudotuberculosis* or MDCK cells that ingested polystyrene beads coated with E-cadherin or transferrin [32].

The Gal/GalNAc-specific lectins, which are implicated in recognition of ligands on the host and bacterial surface [33], were unexpectedly detected at all time points in phagosomes. All subunits of Gal/GalNAc-specific lectin, Hgl, Igl, and Lgl, were constitutively present. In macrophages, neutrophils, and *Dictyostelium* [34], plasma membrane proteins including surface receptors that recognize extracellular materials to initiate phagocytosis, such as the Fcγ [35,36] and mannose phosphate receptors [35], are immediately recycled to the membrane surface after internalization of the materials. The continuous presence of all lectin subunits in *E. histolytica* phagosomes for up to 48 h (data not shown) strongly indicates that these lectin subunits are not simply shuttled between the plasma membrane and the early phagosomes, but might have an unidentified role in phagosome biogenesis.

Three proteins with mitochondrial homologues, two mitochondrial-type Hsp70 homologues and pyridine nucleotide-

Table 1
Kinetics of phagosome proteins identified with LC–MS and MS/MS

TIGR protein ID	NCBI accession number	Protein name (organism source)	Identity (%)	Chase (min)				Detected in three strains[m]
				0	30	60	120	
Vesicular trafficking, other small GTPases, and effectors								
170.m00128	AB054578	Rab1	100	+	−	+	−	○
30.m00257	AB054582	Rab5	100	±	−	+	−	×
333.m00048	AF218311	Rab7A[a,b]	100	+	+	+	+	○
7.m00469	AB186363	Rab7B[a,b]	100	+	±	±	−	×
122.m00143	AB186364	Rab7C[a,b]	100	+	±	−	−	×
141.m00085	AB186365	Rab7D[a,b]	100	+	−	+	−	×
177.m00124	AB186366	Rab7E[a,b]	100	+	+	+	+	○
95.m00153	AF389109	Rab8	100	−	−	+	−	×
105.m00137	AB054587	Rab11B	100	±	+	+	+	○
285.m00064	AB054588	Rab11C	100	−	±	+	−	○
20.m00333	AB197095	RabX17	100	±	±	+	±	○
13.m00301	AB054579	RabC1[c]	100	+	−	+	−	×
78.m00171	AB186371	RabC2[c]	100	−	−	+	−	×
121.m00115	BAD82823	RabC3[c]	100	+	+	+	±	×
179.m00077	U01052	Rap2	100	+	+	+	+	○
34.m00236	EAL49830	δ-Adaptin 3 (*Homo sapiens*)	31	±	±	±	−	×
296.m00052	EAL50512	Clathrin coat assembly protein ap50[a] (*Dictyostelium discoideum*)	48	+	±	+	−	○
18.m00327	EAL50667	COPI α subunit (*Emericella nidulans*)	31	−	−	−	±	×
198.m00123	XP_650820	Guanine nucleotide exchange factor[a] (*Entamoeba dispar*)	26	±	−	±	±	×
64.m00149	EAL48651	Guanine nucleotide exchange factor A (*Dictyostelium discoideum*)	36	−	±	−	−	×
21.m00230	EAL44117	Rab escort protein (*Drosophila melanogaster*)	29	−	−	−	±	×
82.m00147	EAL48069	Ras guanine nucleotide exchange factor[a] (*Dictyostelium discoideum*)	29	−	±	±	±	×
282.m00062	EAL44258	Ras guanine nucleotide exchange factor 2 (*Homo sapiens*)	32	−	±	−	−	○
68.m00228	EAL48551	Receptor mediated endocytosis protein 1[a] (*Caenorhabditis elegans*)	44	±	−	±	−	×
201.m00111	EAL45367	Syntaxin 16[a,d] (*Mus musculus*)	35	+	+	+	+	○
Hydrolytic enzymes								
276.m00059	EAL44332	Acid phosphatase[a] (*Homo sapiens*)	25	+	±	±	−	○
138.m00092	EAL46577	Acid phosphatase[a,e] (*Homo sapiens*)	26	+	±	+	±	○
25.m00244	EAL50253	α-Amylase (*Xanthomonas campestris*)	25	±	±	±	−	○
13.m00352	EAL51020	β-Amylase (*Paenibacillus polymyxa*)	27	±	−	±	−	×
231.m00061	AJ417748	β-Hexosaminidase B	100	+	+	+	+	○
242.m00078	Q01957	Cysteine protease 1	100	+	+	+	+	○
206.m00082	Q01958	Cysteine protease 2	100	+	+	+	+	○
10.m00362	CAA62833	Cysteine protease 4	100	+	±	±	+	○
191.m00117	CAA62835	Cysteine protease 5	100	+	+	+	+	○
4.m00700	EAL51699	Dipeptidase[a] (*Mus musculus*)	42	−	±	−	±	×
33.m00237	AF059278	Dipeptidyl aminopeptidase	100	+	±	±	±	○
297.m00060	EAL44104	Exoribonuclease[a] (*Oryza sativa*)	38	−	−	−	±	×
87.m00172	X87610	Lysozyme 1[a]	100	+	±	+	+	○
6.m00454	AF034843	Lysozyme 2	100	−	+	+	+	○
66.m00168	EAL48609	Phosphodiesterase 3a[a] (*Homo sapiens*)	26	−	−	−	±	×
33.m00231	EAL49871	Phospholipase A_2	100	+	±	+	−	○
304.m00064	XP_649424	Phospholipase B[a,f] (*Dictyostelium discoideum*)	31	+	±	+	±	○
62.m00161	XP_654113	Phospholipase B (*Dictyostelium discoideum*)	27	+	+	+	±	○
223.m00078	XP_650385	Ribonuclease[a] (*Lycopersicon esculentum*)	29	−	−	−	+	×
8.m00375	EAL51377	Serine protease[g] (*Caenorhabditis elegans*)	31	+	±	+	+	×
133.m00131	EAL46703	Serine protease (*Caenorhabditis elegans*)	30	+	+	+	+	○
30.m00222	EAL50008	Surface protease (*Trypanosoma brucei*)	29	±	−	±	−	×
Cytoskeletal proteins								
8.m00351	M16339	Actin	100	+	+	+	+	○
61.m00188	EAL48769	Cortexillin 2[a] (*Polysphondylium pallidum*)	27	−	−	−	±	×

Table 1 (*Continued*)

TIGR protein ID	NCBI accession number	Protein name (organism source)	Identity (%)	Chase (min)				Detected in three strains[m]
				0	30	60	120	
3.m00571	EAL51907	Interaptin[a] (*Dictyostelium discoideum*)	26	−	±	−	±	×
22.m00287	EAL50436	Protovillin (*Dictyostelium discoideum*)	26	−	±	±	±	○
57.m00161	EAL48917	Talin (*Dictyostelium discoideum*)	25	+	±	±	−	○
97.m00135	U29720	RacA	100	+	+	+	+	○
108.m00133	U29722	RacC	100	+	±	+	±	×
16.m00303	U30148	RacD	100	±	−	+	−	×
110.m00118	EAL47274	RacG[h]	100	−	−	+	−	×
146.m00106	AF055340	RacG	100	+	+	+	−	○
Signal transduction								
6.m00493	EAL51590	Calcium-dependent protein kinase 2[a] (*Plasmodium falciparum*)	30	±	−	−	−	×
58.m00154	EAL48877	Ethylene-responsive protein kinase Ctr1[a] (*Lycopersicon esculentum*)	34	−	−	−	±	×
1.m00724	EAL52122	p21-Activated protein kinase (*Dictyostelium discoideum*)	46	+	−	−	−	○
400.m00036	EAL43350	p150 Target of rapamycin (*Mus musculus*)	26	−	±	−	±	×
67.m00099	XP_653966	Receptor-like protein kinase (*Pharbitis nil*)	25	−	−	−	+	×
33.m00227	EAL49867	Rok-α (*Rattus norvegicus*)	25	−	−	−	±	×
11.m00358	AAM21055	Serine/threonine protein kinase	100	−	+	−	−	×
359.m00061	EAL43605	Tmk 39	100	±	−	−	−	×
Lectins and surface proteins								
191.m00115	CAB45102	Aminophospholipid translocase 2b[a] (*Homo sapiens*)	44	±	±	−	−	×
16.m00300	EAL50797	Gal/GalNAc lectin Hgl1–5[a,i]	100	+	+	+	+	○
53.m00171/119.m00118	EAL49060/ EAL47008	Gal/GalNAc lectin lgl1,2[i]	100	+	+	+	+	○
17.m00351/1.m00673	EAL50759/ EAL52074	Gal/GalNAc lectin Lgl1–5[i]	100	+	+	+	+	○
52.m00161	X55028	Immunodominant variable surface antigen	100	±	±	+	+	○
6.m00429	XP_656907	Mannose 6-phosphate receptor (*Xenopus laevis*)	27	+	+	±	+	○
151.m00094	EAL46316	Multidrug resistance protein 2 (*Canis familiaris*)	31	+	±	±	±	○
Calcium and proton pump								
80.m00163	EAL48139	Calcium transporting ATPase[j]	100	+	±	+	−	×
55.m00199	U20321	Calcium transporting ATPase	100	+	−	+	−	×
79.m00136	EAL48176	V-ATPase V0 domain subunit a[a] (*Homo sapiens*)	33	±	−	−	−	×
101.m00122	U01057	V-ATPase V0 domain subunit c	100	−	±	−	+	○
Mitochondria-like proteins								
65.m00150	EAL48267	Mitochondrial-type Hsp70[k] (*Trachipleistophora hominis*)	27	−	−	−	±	×
76.m00153	EAL48631	Mitochondrial-type Hsp70 (*Encephalitozoon hellem*)	29	−	−	−	±	×
490.m00041	U13421	Pyridine nucleotidetranshydrogenase	100	+	+	+	+	○
Other proteins								
84.m00140	XP_653385	Beige protein (*Dictyostelium discoideum*)	37	±	−	−	−	×
50.m00176	EAL49183	β-Ketoacyl-CoA synthase (*Marchantia polymorpha*)	43	−	±	±	−	×
32.m00217	EAL49910	Calcium-binding protein (*Dictyostelium discoideum*)	50	+	+	+	+	○
117.m00153	EAL47096	Catabolic threonine dehydratase (*Thermotoga maritima*)	49	−	±	−	±	×
687.m00017	EAL42583	Copine 1[a,l] (*Oryza sativa*)	45	+	+	+	−	×
24.m00266	EAL50288	Copine 1[a] (*Oryza sativa*)	45	+	−	±	−	×
12.m00301	EAL51089	CRAG protein[a] (*Drosophila melanogaster*)	27	±	−	−	−	×
11.m00359	AF017993	Cyclophilin	100	+	+	+	+	○
143.m00085	M92073	Elongation factor 1-α	100	+	+	+	+	○
160.m00096	EAL46140	Erythrocyte-binding protein 3[a] (*Plasmodium falciparum*)	31	−	−	−	±	×

Table 1 (*Continued*)

TIGR protein ID	NCBI accession number	Protein name (organism source)	Identity (%)	Chase (min)				Detected in three strains[m]
				0	30	60	120	
12.m00311	M89790	Glyceraldehyde-3-phosphate dehydrogenase	100	−	−	−	+	×
147.m00106	EAL46406	Glycogen synthase kinase-3[a] (*Medicago sativa*)	46	±	−	±	−	×
27.m00240	EAL50132	Helicase (*Saccharomyces cerevisiae*)	38	−	−	−	±	×
136.m00105	AAG01040	70 kDa heat shock protein	100	−	−	−	±	×
6.m00440	XP_656918	Lasp protein[a] (*Drosophila melanogaster*)	39	+	−	+	+	×
137.m00092	EAL46601	Phenylalanine-trna synthetase[a] (*Homo sapiens*)	48	±	±	±	−	×
6.m00511	EAL51503	Reverse transcriptase	100	−	+	−	−	×
259.m00048	EAL44546	Rsu-1[a] (*Homo sapiens*)	33	±	±	±	−	×
222.m00074	Z48307	TATA-box-binding protein[a]	100	±	−	−	−	×
50.m00171	EAL49178	Terbinafine resistance locus protein yip1[a] (*Leishmania major*)	36	+	−	±	−	×
34.m00254	X98567	Ubiquitin	100	+	+	+	−	○
277.m00056	EAL44321	Ubiquitin carboxyl-terminal hydrolase[a] (*Gallus gallus*)	30	−	±	−	−	×
64.m00154	EAL48656	Ubiquitin carboxyl-terminal hydrolase 2 (*Mus musculus*)	28	±	−	±	−	×
3.m00624	EAL51869	Werner helicase interacting protein[a] (*Mus musculus*)	43	−	−	−	±	×

We list protein names with organism names in parentheses. Organism names are not indicated when detected peptides perfectly match the previously reported *E. histolytica* proteins. In cases where highest similarity is demonstrated against putative homologs from other organisms, protein names, organism sources in parenthesis, and percentage identities are shown. We show putative protein names in cases, where (1) homologues with known or predicted functions were found and (2) amino acid identity and *E*-value were >25% and $<10^{-5}$, respectively. Proteins with the peptide coverage of >5%, 0.1–5%, or undetected at each time points are marked with "+", "±", "−", respectively.

[a] It indicates annotation used in the NCBI non-redundant database, while the protein is annotated differently in the *E. histolytica* Genome Database at TIGR.

[b] Rab7A shows 26–44% identity to other Rab7 isotypes.

[c] RabC1 shows 34–44% identity to RabC2 and C3.

[d] Syntaxin 16 homolog (201.m00111) also shows significant homology to mouse syntaxin 12, 13, 2, and 7.

[e] Acid phosphatase (276.m00059) shows 14% identity to 138.m00092.

[f] Phospholipase B (304.m00064) shows 8.3% identity to 62.m00161.

[g] Serine protease (8.m00375) shows 16% identity to 133.m00131.

[h] RacG (110.m00118) shows 54% identity to 146.m00106.

[i] Isotypes of Hgl, Igl, and Lgl were not assigned due to high similarity among these isotypes.

[j] Calcium transporting ATPase (80.m00163) shows 83% identity to 55.m00199.

[k] Mitochondrial-type Hsp70 (65.m00150) shows 8% identity to 76.m00153.

[l] Copine 1 (687.m00017) shows 32% identity to 24.m00266.

[m] Circles indicate proteins detected in all three strains (HM1, KU33, and HATAJI); crosses indicate proteins detected in only HM1 or two strains including HM1.

transhydrogenase, were detected and showed distinct kinetics. The two Hsp 70 homologues were detected from the late phagosomes, while transhydrogenase, which possesses a putative mitochondiral targeting signal and is assumed to be localized to the mitosome, a mitochondria-like remnant organelle unique to two anaerobic parasitic protists [37], was constitutively associated with phagosomes. These proteins were not detected in the profile of non-specific binding proteins from the amebic crude lysate [10], reinforcing that they were not contaminants in the purified phagosome samples. Another well-characterized mitosome-associated protein cpn60 [37] was not detected from purified phagosomes by immunoblot analysis (data not shown). These data suggest that mitosomes per se are not associated with phagosome, but that individual mitochondria-like proteins are recruited to phagosomes in the course of phagosome maturation. One of the putative transmembrane kinases which were previously identified as a family of proteins with sequence similarity to the Gal/GalNAc-specific lectin Igl [38], tmk39, was detected at the early phase of phagosome maturation. It suggests that tmk39 may be involved in signal transduction leading to the phagosome formation.

3.4. Confirmation of kinetics of representative phagosome proteins during phagosome maturation by immunoblot analysis

We observed a high degree of variation in the peptide coverage at different time points. For instance, Igl showed peptide coverages of 10, 50, 23, and 48% at 0, 30, 60, and 120 min, respectively (Fig. 3B, a dotted line). In contrast, CP5 showed similar coverage at all times throughout phagosome maturation. Although Rab7A appeared to be constitutively present in phagosomes (Table 1), the peptide coverage varied among the time points (Fig. 3B, a dotted line). Since percentage coverages of the